

Baryon form factors: Model-independent results*

Ulf-G. Meißner^a

^aForschungszentrum Jülich, Institut für Kernphysik (Theorie), D-52425 Jülich, Germany

Baryon form factors can be analyzed in a largely model-independent fashion in terms of two complementary approaches. These are chiral perturbation theory and dispersion relations. I review the status of dispersive calculations of the nucleon electromagnetic form factors in the light of new data. Then, I present the leading one-loop chiral perturbation theory analysis of the hyperon and the strange nucleon form factors. Open problems and challenges are also discussed.

1. Outline

There are many interesting recent theoretical developments concerning the strange and electromagnetic (em) form factors (ffs) of the nucleon and of the hyperons. Although often useful, in this talk I will eschew models and only discuss some largely model-independent results which have emerged over the last years. The pertinent methods are *dispersion relations* and *chiral perturbation theory*. For such a model-independent description, one has of course to pay a price, namely one needs a certain amount of input data. Indeed, dispersion relations make use of all available data and can be applied over the full range of accessible energies. Chiral effective field theories are limited to energies below the typical hadronic scale of about 1 GeV. As I will show, both methods allow to deepen our understanding of hadronic structure. Instead of a general introduction, I will briefly summarize which topics will be addressed in this talk. *(i) Dispersion theory for the nucleon em ffs*: Dispersion relations have been used for many decades to analyze the data on electron-proton (or deuteron) scattering. The status of such calculations as of 1996 is reviewed in the talk [1]. Here, I will briefly discuss the impact of the recent data from MAMI, NIKHEF, BATES and CEBAF on these calculations. *(ii) Hyperon form factors*: Recent measurements of the Σ^- radius using elastic hadron-electron scattering at CERN and Fermilab have triggered a chiral perturbation theory (CHPT) analysis of the hyperon form factors. It seems to indicate that for these observables SU(3) baryon CHPT is indeed a very *effective* method. *(iii) Strangeness in the nucleon*: Recent data from MIT-BATES and Jefferson Lab allow for a complete leading one-loop analysis of the strange nucleon form factors in the framework of baryon CHPT. This has been attempted before but could not be done due to the lack of data. In the following, I will address these questions and outline further directions of theoretical research.

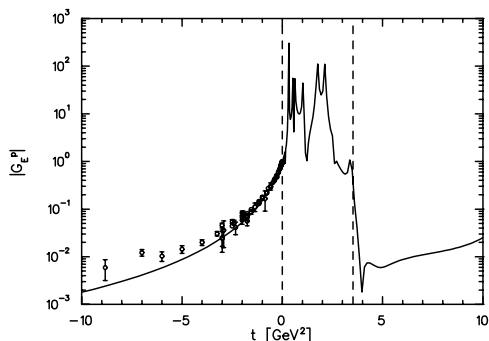
*Plenary talk presented at "Nucleon '99", Frascati, Italy, June 7-9, 1999.

2. Dispersion relations update

The structure of the nucleon as probed with virtual photons is parametrized in terms of four form factors. One can either choose the basis of the Dirac and Pauli ffs ($F_{1,2}(t)$), or equivalently, the so-called Sachs (electric and magnetic) ffs ($G_{E,M}(t)$), with $t = q^2 = -Q^2$ the invariant momentum transfer squared (note that $t < 0$ in electron scattering). In the Breit frame, the Sachs form factors give the distribution of charge and magnetization within the proton and the neutron. The neutron electric ff plays a particular role since the neutron charge is zero, but still there is a non-vanishing distribution of charge which leads to the non-vanishing but small ff. Although not proven strictly (but shown to hold in all orders in perturbation theory), one can write down an unsubtracted dispersion relation for $F(t)$ (which is a generic symbol for any one of the four ff's),

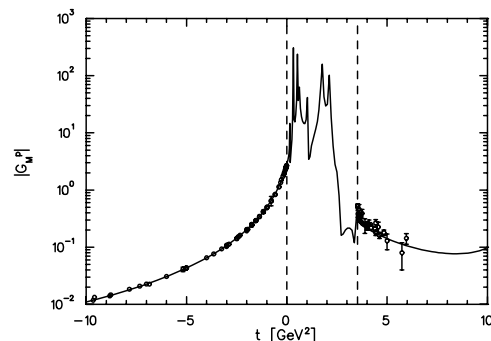
$$F(t) = \frac{1}{\pi} \int_{t_0}^{\infty} dt' \frac{\text{Im} F(t')}{t' - t}, \quad (1)$$

with t_0 the two (three) pion threshold for the isovector (isoscalar) ffs. $\text{Im} F(t)$ is called the *spectral function*. It is advantageous to work in the isospin basis, $F_i^{I=0,1} = (F_i^p \pm F_i^n)/2$, since the photon has an isoscalar ($I = 0$) and an isovector ($I = 1$) component. In general, the spectral functions can be thought of as a superposition of vector meson poles and some continua, related to n-particle thresholds, like e.g. 2π , 3π , $K\bar{K}$, $N\bar{N}$ and so on. For example, in the Vector Meson Dominance (VMD) picture, one simply retains a set of poles. This turns out to be an insufficient approximation. The dispersive approach of refs.[3,4] includes three (or four) isoscalar and three isovector poles. Unitarity allows to reconstruct the isovector spectral functions up to $t \simeq 1 \text{ GeV}^2$ and this model-independent piece contains the ρ . In addition, perturbative QCD behaviour plus some other refinements can be built in. The proton electric and magnetic form factors in the space- and time-like as well as in the unphysical region ($0 \leq t \leq 4m^2$, with m the nucleon mass) for this fit are shown in figs.1,2. It should be pointed out that for the existing data scaling as predicted by pQCD is not yet observed, in particular for the ratio $Q^2 F_2^p(Q^2)/F_1^p(Q^2)$ below $Q^2 = 10 \text{ GeV}^2$. In that region, there is still a sizeable vector meson pole contribution. Recently, a different dispersive approach has been presented which allows for a consistent



14-0411997 15-05-20

f11a 0037.PDF



14-0411997 15-05-02

f11a 0037.PDF

Figure 1. Dispersive analysis of the electric proton form factor (solid line).

Figure 2. Dispersive analysis of the magnetic proton form factor (solid line).

description of the time- and space-like data but less theoretical constraints are built in [5]. Most interesting is the appearance of a resonance-like structure just below the two-nucleon threshold in the description of the neutron data. An interpretation in terms of a dibaryon could be possible, but clearly this phenomenon deserves more study. It would also be interesting to see a refined version of this calculation.

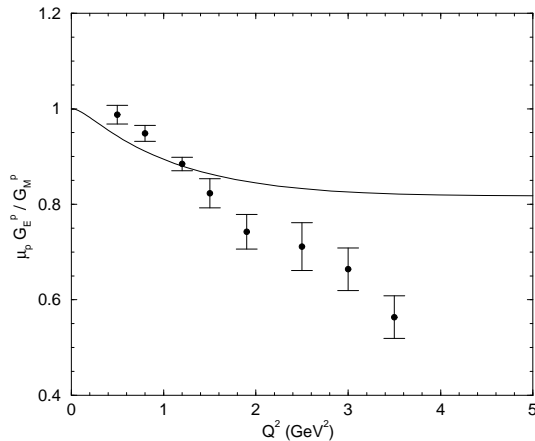


Figure 3. The ratio $\mu_p G_E^p(Q^2)/G_M^p(Q^2)$ as measured at Jefferson Lab. The solid line is the result of a dispersive analysis of *all* data on *all* nucleon form factors. For further discussions, see the text.

Since the time of ref.[1], new data for the ratio of the protons electric and magnetic form factors have been obtained at CEBAF using polarization transfer [2] (for Q^2 between 0.5 and 3.5 GeV²). These data are much more precise than previous ones since the Rosenbluth separation is avoided. They are shown in fig.3. The solid line gives the result of the dispersive analysis with at most three isovector and four isoscalar poles. Even if one decreases the experimental errors to zero, the result of the fit does not change. I conclude that in the *ansatz* for the spectral functions an essential physics ingredient is missing. Whether this can be remedied by the inclusion of further poles or a better treatment of continua (beyond the two-pion continuum) is an open problem which requires more theoretical work.

The situation concerning the neutron electric form factor is not yet satisfactory. The extraction of this quantity from elastic electron scattering off the deuteron was claimed to be plagued by a strong dependence on the deuteron wavefunction [6], as shown in fig.4 by the thin dotted lines. However, in view of the fact that all modern two-nucleon potentials give the same results for a huge amount of two- and three-nucleon observables, this wavefunction dependence is presumably an artefact of the treatment in ref.[6]. A modern extraction from the same data based on the Argonne V18 potential is shown by the open circles in fig.4 [7]. Also shown are the recent data from BATES, MAMI and NIKHEF [8]. These measurements invoke polarized targets or polarization transfer and thus have much less systematic uncertainties. Still, the error bars are sizeable. Note that these new data tend to give larger values for the neutron electric form factor, with the exception of the two points at $Q^2 = 0.32$ and 0.36 GeV² obtained with the help of a polarized ³He target. The solid line in that figure is the result of the dispersive analysis. We took the Saclay data as given by the Paris potential but doubled the error bars to account for the wavefunction dependence. A systematic treatment of these data using all available high precision potentials and consistent exchange currents is called for. I expect that such an investigation will lead to a sizeably reduced wavefunction dependence (if there

is any). Of course, a reduction of the error bars for the polarization data would also be helpful to further pin down the neutron electric form factor. In particular, there is still the discrepancy between the deuteron and the helium points to be resolved.

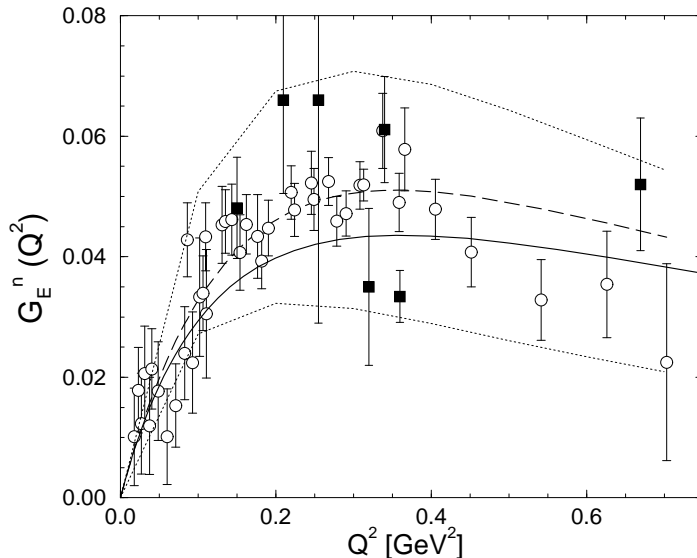


Figure 4. The neutron electric form factor. For explanations, see the text.

3. Hyperon form factors

To third order in the chiral expansion, i.e. to leading one-loop order, the electromagnetic form factors of the nucleon have been studied in refs.[10–12]. At that order, one has to deal with two counterterms in the electric and two in the magnetic ffs. Using e.g. the proton and neutron electric radii and magnetic moments as input, the ffs are fully determined to that order. In particular, no counterterms appear in the momentum expansion of the magnetic ffs. To this order in the chiral expansion, the ffs are precisely described for momentum transfer squared up to $Q^2 \simeq 0.2 \text{ GeV}^2$. It appears therefore natural to extend such an investigation to the three flavor case. Surprisingly, that has never been attempted until recently [9] despite a huge amount of studies in three flavor chiral perturbation theory. This investigation was triggered by the recent results on the Σ^- radius obtained by the WA89 collaboration at CERN and by the SELEX collaboration at FNAL (note that the SELEX results are still preliminary),

$$\langle r_{\Sigma^-}^2 \rangle_{\text{exp}} = 0.92 \pm 0.32 \pm 0.40 \text{ fm}^2 [14], \quad \langle r_{\Sigma^-}^2 \rangle_{\text{exp}} = 0.60 \pm 0.08 \pm 0.08 \text{ fm}^2 [15], (2)$$

obtained by scattering a highly boosted hyperon beam in the electronic cloud of a heavy atom (elastic hadron–electron scattering). The pattern of the charge radii embodies information on SU(3) breaking and the structure of the groundstate octet. In a CHPT calculation of the corresponding ffs, the baryon structure is to some part given by the meson (pion and kaon) cloud and in part by shorter distance physics parametrized in terms of local contact interactions. In the general case, such a splitting depends on the regulator

scheme and scale one chooses. Here, we work in standard dimensional regularization and set $\lambda = 1 \text{ GeV}$ throughout (since this is the natural hadronic scale). If one performs the SU(3) calculation to third order, one has no new counterterms as compared to the SU(2) calculation. Therefore, fixing the low-energy constants (LECs) from proton and neutron properties allows one to make parameter-free predictions for the hyperons. As an added bonus, kaon loops induce a momentum dependence in the isoscalar magnetic form factor of the nucleon, as first pointed out in ref.[13], whereas in the pure SU(2) calculation, $G_M^{I=0}(Q^2)$ is simply constant. This allows one to study the contribution of kaon loops (strangeness) to the em ffs of the nucleon (not to be confused with the strange ffs to be discussed below).

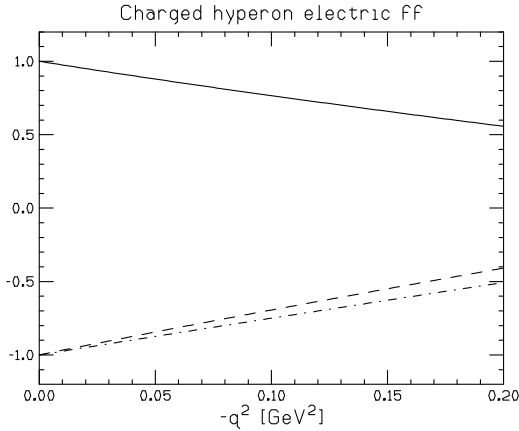


Figure 5. The electric form factors of the charged hyperons calculated in three flavor baryon CHPT. Solid, dashed, dot-dashed line: Σ^+ , Σ^- , Ξ^- , in order.

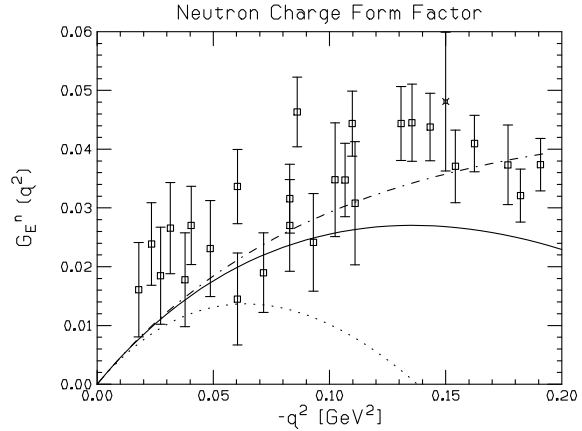


Figure 6. Electric neutron form factor calculated within SU(3) (solid line) and SU(2) (dotted line). The dot-dashed line is the result of the dispersive analysis, cf. fig.4.

Consider first the hyperons. The electric ffs of the charged hyperons are given in fig.5. The corresponding radii are (a more detailed discussion also of the neutral particles and magnetic radii is given in [9])

$$\langle r_{\Sigma^+}^2 \rangle = 0.64 \dots 0.66 \text{ fm}^2, \quad \langle r_{\Sigma^-}^2 \rangle = 0.77 \dots 0.80 \text{ fm}^2, \quad \langle r_{\Xi^-}^2 \rangle = 0.61 \dots 0.65 \text{ fm}^2. \quad (3)$$

The given uncertainty does not reflect the contribution from higher orders, which should be calculated. The prediction for the Σ^- is in fair agreement with the recent measurements. The result for the Σ radii is at variance with quenched lattice QCD calculations which give $0.56(5) \text{ fm}^2$ and $0.72(6) \text{ fm}^2$ for the negative and positive Σ , respectively [16]. However, quenched lattice calculations should be taken with a grain of salt (the true error due to the quenching is only known for very few quantities, certainly not for the radii). In the CHPT approach, the difference of the radii is due to some short distance physics

encoded in the LEC d_{102}^0 and to the Foldy term. The loop contributions are almost equal, but the difference due to the counterterm and the Foldy term for the Σ hyperons is

$$\langle r_{\Sigma^+}^2 \rangle - \langle r_{\Sigma^-}^2 \rangle = -\frac{8d_{102}}{(4\pi F_\phi)^2} + \frac{b_D}{m^2} = -0.10 \dots - 0.15 \text{ fm}^2, \quad (4)$$

depending on how one fixes the electric LEC d_{102} and the magnetic LEC b_D . Here, $F_\phi = 100 \text{ MeV}$ is the average pseudoscalar decay constant. A more detailed discussion of the parameter dependence is given in [9]. All the numbers given here are based on a third order calculation. Clearly, a fourth order calculation is called for to further quantify these results.

As can be seen from fig.6, the chiral description of the neutron charge ff is clearly improved in SU(3) (solid line) as compared to the two flavor case (dotted line). Obviously, this sizeable kaon cloud effect will be reduced at next order since the effect of recoil only starts to show up at fourth order. The inclusion of such recoil effects is expected to improve already the SU(2) calculation, leaving less room for the kaon cloud effects. It is also worth pointing out that this effect from kaon loops is opposite to what one expects from a ϕ -coupling [17] and thus some cancellations should take place.

4. Strange vector form factors

Recently, the first results from parity-violating electron scattering experiments, which allow to pin down the so-called strange form factors of the nucleon, have become available. These strange ffs parametrize the matrix elements of the strange vector current,

$$\langle N | \bar{s} \gamma_\mu s | N \rangle = \langle N | \bar{q} \gamma_\mu (\lambda^0/3 - \lambda^8/\sqrt{3}) q | N \rangle, \quad (5)$$

with $q = (u, d, s)$ denoting the triplet of the light quark fields and $\lambda^0 = I$ (λ^a) the unit (the $a = 8$ Gell-Mann) SU(3) matrix. The singlet and octet currents are parametrized in terms of electric and magnetic ffs, which give the strange ffs via

$$G_{E/M}^{(s)}(Q^2) = G_{E/M}^{(s)}(0) + \frac{1}{6} \langle r_{E/M,s}^2 \rangle Q^2 + \mathcal{O}(Q^4). \quad (6)$$

The SAMPLE collaboration has reported the first measurement of the strange magnetic moment of the proton [18]. To be precise, they give the strange magnetic form factor in units of nuclear magnetons at a small momentum transfer $Q_S^2 = 0.1 \text{ GeV}^2$, $G_M^{(s)}(Q_S^2) = +0.23 \pm 0.37 \pm 0.15 \pm 0.19$. The rather sizeable error bars document the difficulty of such type of experiment. The HAPPEX collaboration has chosen a different kinematics which is more sensitive to the strange electric form factor [19]. Their measurement implies $G_E^{(s)}(Q_H^2) + 0.39 G_M^{(s)}(Q_H^2) = 0.023 \pm 0.034 \pm 0.022 \pm 0.026$, at $Q_H^2 = 0.48 \text{ GeV}^2$. Of course, this momentum transfer might be too high for the CHPT analysis at third order to hold, but in the absence of data at lower Q^2 let us assume that we can still use the HAPPEX result. This loophole should be kept in mind. There have been many theoretical speculations about the size of the strange form factors, some of them clearly in conflict with the data. These data have been analyzed in the framework of chiral perturbation theory [20], extending previous work [21]. It was shown in [13] that one can make a parameter-free prediction for the momentum dependence of the nucleons' strange

magnetic (Sachs) form factor based on the chiral symmetry of QCD solely. The value of the strange magnetic moment, which contains an unknown low-energy constant (b_0), can be deduced from the SAMPLE experiment using the momentum-dependence derived in [13]. Furthermore, the SU(3) analysis of the octet electromagnetic form factors performed in [9] allows one to pin down the octet component of the strange vector current. Thus, to leading one-loop order, there is only one new singlet counterterm (d_{102}^0), the strength of which can be determined from the value found by HAPPEX. This allows to give a band for the strange electric form factor and make a prediction for the MAMI A4 experiment, which intends to measure $G_E^{(s)}(Q_M^2) + 0.22 G_M^{(s)}(Q_M^2)$ with a four-momentum transfer (squared) $Q_M^2 = 0.23 \text{ GeV}^2$ of approximately half the HAPPEX value. Under the assumptions mentioned, one can determine the LECs b_0 and d_{102}^0 with sizeable uncertainties reflecting the experimental input. The central values are of natural size and the corresponding results for the strange electric and magnetic ff are shown in figs.7,8 by the solid lines. The dashed lines reflect the theoretical uncertainty based on a very conservative analysis. The corresponding strange radii and the strange magnetic moment are [13,20]

$$\langle r_{E,s}^2 \rangle^{1/2} = (0.05 \pm 0.09) \text{ fm}^2, \quad \langle r_{M,s}^2 \rangle^{1/2} = -0.14 \text{ fm}^2, \quad \mu_s = (0.18 \pm 0.44) \text{ n.m.}, \quad (7)$$

where the uncertainty in the strange radius stems mostly from the uncertainty in the singlet LEC d_{102}^0 , whereas the prediction for the magnetic radius at this order is parameter-free. The uncertainty in μ_s is completely given by the error of the SAMPLE analysis. A few more remarks on the strange electric ff are in order. The radius is fairly small

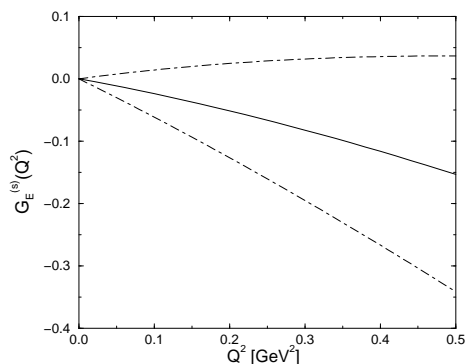


Figure 7. The strange electric form factor from chiral perturbation theory.

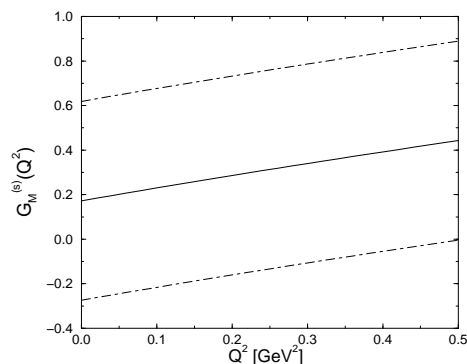


Figure 8. The strange magnetic form factor from chiral perturbation theory.

and *positive*, and even given the sizeable uncertainty, it is on the lower side of the predictions based on dispersive approaches including maximal OZI violation [22,23]. It is more compatible with models that include $\pi\rho$ [24] contributions in the isoscalar spectral functions besides the vector meson poles (ω, ϕ, \dots) or dispersive analysis of the $\bar{K}K$ [25] continuum. Note also that from the octet current the strange electric radius inherits the chiral singularity $\sim \ln(M_K)$. It is also worth pointing out that the momentum dependence of the strange electric form factor is rather different from the one of the neutron

charge form factor, which also vanishes at zero momentum transfer. We also note that using the central values for the LECs, the prediction for the MAMI A4 experiment, which attempts to measure $G_E^{(s)}(Q_M^2) + 0.22 G_M^{(s)}(Q_M^2)$ at a four-momentum transfer (squared) of $Q_M^2 = 0.23 \text{ GeV}^2$, is very small but afflicted with a large uncertainty. A more detailed discussion is given in ref.[20]. It is also important to stress that a dispersive analysis of the $K\bar{K}$ continuum leads to much smaller values for the strange radii [26]. That approach is based on an analytic continuation of the empirical KN scattering amplitudes and unitarity bounds are used. In principle, CHPT calculations and dispersion relations can be mapped one-to-one as has been shown, see e.g. ref.[27]. Both calculations need to be improved. On the CHPT side, the next order has to be investigated in order to check the convergence. The dispersion relations need better data, since the analytic continuation so far cannot be made stable without extra assumptions. More direct data from Jefferson Lab and MAMI should help to clarify the situation.

5. Electromagnetic nucleon–delta transition form factors

Recently, a consistent scheme to include the $\Delta(1232)$ in a chiral effective field theory was set up [31]. It is based on the observation that the $N\Delta$ mass splitting $\delta = m_\Delta - m_N$ is only 300 MeV and that the Δ is coupled strongly to the $N\pi\gamma$ system. Treating the mass splitting as an additional small parameter, one then expands in external momenta, pion mass insertions *and* δ (all divided by the hadronic scale of 1 GeV). One collectively denotes these small parameters as ϵ . This so-called small scale expansion is a phenomenological extension of CHPT. In ref.[32], the isovector $N\Delta$ –transition was calculated to third order in ϵ . The transition matrix element is parametrized in terms of three form factors $G_{1,2,3}(Q^2)$. To that order, one has only two non-vanishing and finite loop diagrams and all counterterms are momentum-independent. That means that the Q^2 –dependence of the transition ffs is predicted in a parameter-free way and thus is a good testing ground for chiral dynamics. Since the intermediate πN state can go on mass-shell, these ffs are complex, even at $Q^2 = 0$. That is not accounted for in most models. These ffs can be mapped uniquely onto the multipole amplitudes $M_1(Q^2)$, $E_2(Q^2)$ and $C_2(Q^2)$. Consequently, the Q^2 –dependence of the EMR E_2/M_1 and of the CMR C_2/M_1 can be predicted. In figs.9,10 the momentum dependence of the EMR and CMR is shown. The various lines refer to the multipole analysis of the Mainz, RPI and VPI groups, which are used to pin down the LECs at $Q^2 = 0$. A more detailed discussion of these topics can be found in ref.[32]. It will be important to confront the recent measurements from ELSA and BATES with these predictions.

6. Challenges

To my opinion, there are three major issues to be resolved:

- ★ The dispersive analysis relies on a set of precise and consistent data, otherwise the spectral functions can not be extracted without severe assumptions. Clearly, the new data on the ratio $\mu_p G_E^p(Q^2)/G_M^p(Q^2)$ cannot be explained for the type of spectral functions used so far, consisting of a set of vector meson poles, the 2π –continuum and pQCD constraints. I would strongly encourage studies implementing

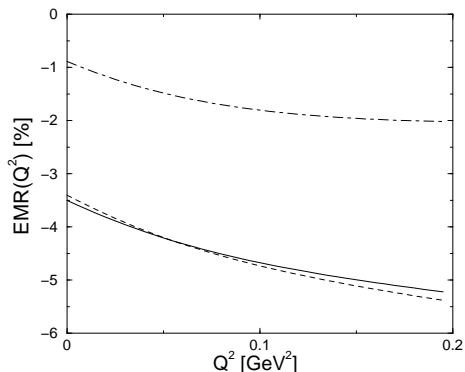


Figure 9. The ratio E_2/M_1 versus Q^2 . The solid, dashed and dot-dashed line refer to input from the Mainz, RPI and VPI multipole analysis, in order.

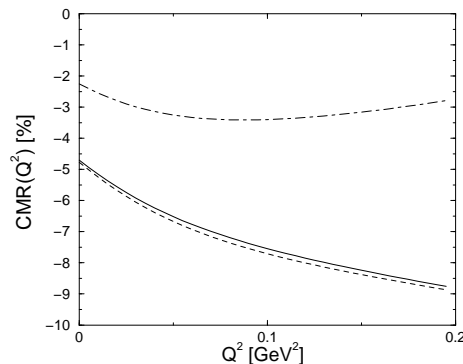


Figure 10. The ratio C_2/M_1 versus Q^2 . The solid, dashed and dot-dashed line refer to input from the Mainz, RPI and VPI multipole analysis, in order.

other continua or correlated multi-meson intermediate states in a consistent manner. Such approaches have been proven to be fruitful in the study of baryon-baryon interactions.

- ★ A fourth order one-loop calculation of the electromagnetic form factors of the baryon octet is mandatory. Such type of calculation has already helped to deepen our understanding of the octet magnetic moments, see ref.[28]. In particular, investigations of recoil effects in the neutron electric form factor and the pattern of the hyperon charge radii are of interest. A recently proposed Lorentz-invariant formulation of baryon CHPT might prove to be a good tool [29].
- ★ More theoretical work is needed to get a better handle on the matrix elements of the strange vector current. With more data particularly at low Q^2 , a fourth order CHPT calculation can be attempted and the effects of the spin-3/2 decuplet should be investigated [30]. Furthermore, the apparent discrepancy between the chiral prediction and the one based on dispersion relations for the strange magnetic radius needs to be resolved.

Finally, it is important to stress that all these problems are intertwined. For example, the extraction of the strange ffs from parity-violation experiments can only be done precisely if the data are accurate enough but also the non-strange ffs are known precisely, since in most parity-violation experiments the latter are used as amplification factors.

Acknowledgements

It is a pleasure to thank my collaborators Véronique Bernard, Harold Fearing, Hans-Werner Hammer, Thomas Hemmert, Bastian Kubis and Sven Steininger. Useful comments and communications from George Gellas, Murray Moinester, Michael Ostrick and Bob Wiringa are also acknowledged.

REFERENCES

1. Ulf-G. Meißner, Nucl. Phys. A623 (1997) 340c.
2. R.D. Ransome, these proceedings.
3. P. Mergell, Ulf-G. Meißner and D. Drechsel, Nucl. Phys. A596 (1996) 367
4. H.-W. Hammer, Ulf-G. Meißner and D. Drechsel, Phys. Lett. B385 (1996) 343
5. R. Baldini et al., Eur. Phys. J. C (1999), in press.
6. S. Platchkov et al., Nucl. Phys. A510 (1990) 740
7. R.B. Wiringa, private communication.
8. T. Eden et al., Phys. Rev. C50 (1994) R1749; M. Meyerhoff et al., Phys. Lett. B327 (1994) 201; C. Herberg et al, Eur. Phys. J. A5 (1999) 131; I. Passchier et al., Phys. Rev. Lett. 82 (1999) 4988; M. Ostrick et al., Phys. Rev. Lett., in press; D. Rohe et al., submitted to Phys. Rev. Lett., J. Becker et al., submitted to Eur. Phys. J.
9. B. Kubis, T.R. Hemmert and Ulf-G. Meißner, Phys. Lett. B456 (1999) 240.
10. J. Gasser, M.E. Sainio and A. Švarc, Nucl. Phys. B307 (1988) 779.
11. V. Bernard, N. Kaiser, J. Kambor and Ulf-G. Meißner, Nucl. Phys. B388 (1992) 315.
12. V. Bernard, H.W. Fearing, T.R. Hemmert and Ulf-G. Meißner, Nucl. Phys. A635 (1998) 121.
13. T.R. Hemmert, Ulf-G. Meißner and S. Steininger, Phys. Lett. B437 (1998) 184.
14. M.I. Adamovich et al. (The WA89 Collaboration), Eur. Phys. J. C 8 (1999) 55.
15. I. Eschrich (SELEX collaboration), **hep-ex/9811003**.
16. D.B. Leinweber et al., Phys. Rev. D43 (1991) 1659.
17. M.F. Gari and W. Krümpelmann, Phys. Lett. B274 (1992) 279.
18. B. Mueller et al. (SAMPLE collaboration), Phys. Rev. Lett. 78 (1997) 3824.
19. K.A. Aniol et al. (HAPPEX collaboration), Phys. Rev. Lett. 82 (1999) 1096.
20. T.R. Hemmert, B. Kubis and Ulf-G. Meißner, **nucl-th/9904076**, Phys. Rev. C (1999), in print.
21. M.J. Ramsey-Musolf and H. Ito, Phys. Rev. C55 (1997) 3066.
22. R.L. Jaffe, Phys. Lett. B229 (1989) 275.
23. H.-W. Hammer, Ulf-G. Meißner and D. Drechsel, Phys. Lett. B367 (1996) 323.
24. Ulf-G. Meißner, V. Mull, J. Speth and J.W. Van Orden, Phys. Lett. B408 (1997) 381.
25. M.J. Ramsey-Musolf and H.-W. Hammer, Phys. Rev. Lett. 80 (1998) 2539; H.-W. Hammer and M.J. Ramsey-Musolf, **hep-ph/9903367**.
26. H.-W. Hammer and M.J. Ramsey-Musolf, **hep-ph/9812261**.
27. J. Gasser and Ulf-G. Meißner, Nucl. Phys. B357 (1991) 90.
28. Ulf-G. Meißner and S. Steininger, Nucl. Phys. B499 (1997) 349.
29. T. Becher and H. Leutwyler, Eur. Phys. J. C9 (1999) 643.
30. S. Puglia and M. Ramsey-Musolf, in preparation.
31. T.R. Hemmert, B.R. Holstein and J. Kambor, J. Phys. G: Nucl. Part. Phys. 24 (1998) 1831.
32. G.C. Gellas et al., Phys. Rev. D60 (1999) 054022.